



King Saud University
Arabian Journal of Chemistry

www.ksu.edu.sa
www.sciencedirect.com



ORIGINAL ARTICLE

Preparation and characterization of gold nanoparticles prepared with aqueous extracts of *Lamiaceae* plants and the effect of follow-up treatment with atmospheric pressure glow microdischarge

Anna Dzimitrowicz^a, Piotr Jamróz^{a,*}, George C. diCenzo^b, Iwona Sergiel^c, Tomasz Kozlecki^d, Pawel Pohl^a

^a Wroclaw University of Technology, Faculty of Chemistry, Department of Analytical Chemistry and Chemical Metallurgy, Wybrzeze Stanislawa Wyspianskiego 27, 50-370 Wroclaw, Poland

^b McMaster University, Department of Biology, 1280 Main St. W., Hamilton, Ontario, Canada

^c University of Zielona Gora, Faculty of Biological Sciences, Department of Biotechnology, Prof. Z. Szafrana 1, 65-516 Zielona Gora, Poland

^d Wroclaw University of Technology, Faculty of Chemistry, Department of Chemical Engineering, Wybrzeze Stanislawa Wyspianskiego 27, 50-370 Wroclaw, Poland

Received 18 January 2016; accepted 7 April 2016

KEYWORDS

Natural plant extracts;
Gold nanoparticles;
Phenolic compounds;
Biosynthesis;
Atmospheric pressure discharge

Abstract The unique properties of gold nanoparticles (AuNPs) make them attractive for use in a number of fields, ranging from cosmetology to medicine. If AuNPs are to be widely used in industrial and medical applications, it is necessary to develop environmentally friendly methods for their synthesis. This can be accomplished by replacing the traditional chemical compounds for the reduction of the Au(III) ions to Au⁰ during AuNPs synthesis with natural plant extracts or with atmospheric pressure plasmas. Here, the properties of three aqueous plant extracts (*Mentha piperita*, *Melissa officinalis*, and *Salvia officinalis*) in the synthesis of AuNPs were compared and optimized under standardized conditions. The effects of the type of plant extract, the reaction temperature, and the precursor concentration on the production and size of the obtained AuNPs were examined using UV–Vis absorption spectrophotometry, dynamic light scattering (DLS), scanning electron microscopy (SEM), and transmission electron microscopy (TEM). It was observed that the size

* Corresponding author. Tel.: +48 71 320 3807; fax: +48 71 320 2494.

E-mail address: piotr.jamroz@pwr.wroc.pl (P. Jamróz).

Peer review under responsibility of King Saud University.



Production and hosting by Elsevier

<http://dx.doi.org/10.1016/j.arabjc.2016.04.004>

1878-5352 © 2016 The Authors. Production and hosting by Elsevier B.V. on behalf of King Saud University.

This is an open access article under the CC BY-NC-ND license (<http://creativecommons.org/licenses/by-nc-nd/4.0/>).

Please cite this article in press as: Dzimitrowicz, A. et al., Preparation and characterization of gold nanoparticles prepared with aqueous extracts of *Lamiaceae* plants and the effect of follow-up treatment with atmospheric pressure glow microdischarge. Arabian Journal of Chemistry (2016), <http://dx.doi.org/10.1016/j.arabjc.2016.04.004>

of the produced AuNPs was dependent on the aqueous plant extract used, and that under the optimized conditions, the aqueous leaf extract of *M. piperita* resulted in the production of AuNPs with the smallest volume-weighted diameter. Additionally, the bioactive compounds present in each extract were studied. Attenuated total reflection Fourier transform infrared spectroscopy (ATR-FTIR) indicated that different chemical groups could be involved in the AuNPs synthesis, while a Folin–Ciocalteu (FC) assay revealed a clear role of phenolic compounds. Finally, it was shown that the treatment of the synthesized AuNPs, which were obtained after bioreduction using the plant extracts, with atmospheric pressure glow microdischarge (μ APGD) resulted in their agglomeration and enlargement.

© 2016 The Authors. Production and hosting by Elsevier B.V. on behalf of King Saud University. This is an open access article under the CC BY-NC-ND license (<http://creativecommons.org/licenses/by-nc-nd/4.0/>).

1. Introduction

Since the early 20th century, the synthesis of gold nanoparticles (AuNPs) has fascinated the scientific community due to their unique physicochemical and biological properties (Link and El-Sayed, 1999; Daniel and Astruc, 2004). It is because of these special properties that many research groups have attempted to use AuNPs to address societally important problems in a range of fields, including medicine (Cole et al., 2015), cosmetology (Saha et al., 2011), biology (Murphy et al., 2008), clinical chemistry (Jain, 2007), and pharmacology (Hainfeld et al., 2008). As such, it is imperative to develop improved and environmentally friendly methods for the synthesis of AuNPs in order to maximize their potential benefits to society. Over the years, there has been a marked improvement in the ability to synthesize AuNPs. However, conventional methods normally involve the use of toxic compounds that are not appropriate for long-term environmental sustainability.

The critical step in the synthesis of AuNPs is the reduction of the Au(III) ions to their metallic form (Au^0). This is most commonly carried out with a chemical reduction method using various chemical reducing agents such as citric acid (Das et al., 2012), borohydride (Olesiak-Banska et al., 2012), or tetrafluoroborate (Wei and Liu, 2011). In addition, chemical stabilizers, e.g., polyvinylpyrrolidone (Wei and Liu, 2011; Dzimitrowicz et al., 2015a), poly(vinyl alcohol) (Dzimitrowicz et al., 2015a; Pimpang and Choo-pun, 2011), or sodium dodecyl sulfate (Saito et al., 2009), are added to the reaction mixtures to prevent uncontrolled growth and sedimentation of AuNPs. The inclusion of the reducing agents and/or stabilizers not only decreases the purity of the obtained AuNPs, but these compounds can be environmentally hazardous. To overcome this limitation, alternative green reduction methods have been developed to replace the chemical reduction step in the AuNP synthesis. These methods involve, for example, the reduction of the Au(III) ions either with non-equilibrium atmospheric pressure plasmas (APPs) (Yan et al., 2014; Heo and Lee, 2011; Bratescu et al., 2011) or with phytochemical compounds (natural plant extracts) (Khalil et al., 2012; Pasca et al., 2014; Joseph and Mathew, 2014; Rajathi et al., 2014; Alam et al., 2014; Basavegowda et al., 2014; Sharma et al., 2014; MubarakAli et al., 2011; Fierascu et al., 2010).

Two groups of plasma-based reduction methods have been developed for the synthesis of AuNPs. In the first group, APP is generated directly in the liquid between two metallic electrodes that are dipped into solutions containing the AuNPs precursor (Bratescu et al., 2011; Hieda et al., 2008; Cho et al., 2011). In the second group, AuNPs are produced at the interface of the APP gaseous microjets with the liquids containing HAuCl_4 (Dzimitrowicz et al., 2015a,b; Tochikubo et al., 2014; Shirai et al., 2014). The most recent of these methods (Dzimitrowicz et al., 2015a,b), and the only one to employ a continuous-flow mode protocol, uses a low power, direct current atmospheric pressure glow microdischarge (dc- μ APGD) for the reduction of the AuNPs precursor. Briefly, in this method, the Au(III) ions are

reduced in a dc- μ APGD based reactor that consists of an Ar nozzle microjet functioning as the anode and a flowing liquid cathode.

An alternative green chemistry method involves the reduction of the Au(III) ions by natural compounds present in the plant extracts (Khalil et al., 2012; Pasca et al., 2014). The reduction via natural compounds is advantageous over the traditional chemical reduction due to the purity, biocompatibility, and environmental compatibility of the produced AuNPs (Pasca et al., 2014; Joseph and Mathew, 2014; Alam et al., 2014). A wide variety of natural plant extracts have been tested in reference to their ability to synthesize AuNPs (Pasca et al., 2014; Joseph and Mathew, 2014; Rajathi et al., 2014; Alam et al., 2014; Basavegowda et al., 2014; Sharma et al., 2014). In order to utilize the natural plant extracts for the AuNPs synthesis at an industrial scale, the target plants should be easy to grow with a high yield, and cheap to cultivate and harvest, while the produced AuNPs should be of a sufficiently high quality. The members of the *Lamiaceae* family of the flowering plants, which includes 7 sub-families and over 7000 plant species, provide many potential candidates that meet the above characteristics. Additionally, previous studies have illustrated the potential of two species of the *Nepetoideae* subfamily, *Mentha piperita* and *Salvia officinalis*, to produce the high quality AuNPs (MubarakAli et al., 2011; Fierascu et al., 2010). For example, MubarakAli et al. (2011) found that a mixture of the *M. piperita* leaf extract and a HAuCl_4 solution incubated above 28 °C for 24 h led to the synthesis of the spherical AuNPs with a dimension of ~ 150 nm. The obtained AuNPs exhibited a strong antibacterial activity against *Escherichia coli* and *Staphylococcus aureus* (MubarakAli et al., 2011). Fierascu et al. (2010) compared the influence of the extracts of *S. officinalis* leaves and flowers, as well as the effect of irradiation by sunlight, on the efficiency of the AuNPs production. The best conditions for the AuNPs synthesis were established to be when the flower extract was used and with exposure of the reaction mixtures to sunlight irradiation (Fierascu et al., 2010). However, to the best of our knowledge, no study has compared the AuNPs synthesis properties of the extracts from different plants of the *Lamiaceae* family under standardized conditions.

The main objective of the present work was to examine the AuNPs synthesis capabilities of leaf extracts from three members of the *Lamiaceae* family under controlled conditions, and determine which one shows the greatest promise for the further study. The tested plants were *M. piperita*, *S. officinalis*, and *Melissa officinalis*, a third member of the *Nepetoideae* subfamily that has not previously been examined in relation to the synthesis of NPs. The effect of these three extracts and the reaction conditions on the optical and granulometric properties of the obtained AuNPs, as well as their synthesis rate, was determined. Furthermore, the aqueous leaf extracts were characterized to gain clues into which compounds function as the bioactive components for the biosynthesis of AuNPs, and then the specific role of the phenolic compounds was further examined. Finally, it was examined whether the application of dc- μ APGD to the AuNPs synthesized with the natural plant extracts would result in a reduction in the size of the AuNPs.

2. Material and methods

2.1. Preparation of aqueous plant extracts

The leaves of three plants, *M. officinalis* (FLOS, Mokrsko, Poland), *S. officinalis* (FLOS, Mokrsko, Poland) and *M. piperita* (KAWON, Gostyn, Poland), were washed and then air-dried. The plant material (leaves) was homogenized in a mortar and then sieved using a 3.2 mm sieve. In order to obtain 1% (m/v) aqueous plant leaf extracts, portions (1.0 g) of the plant powders were mixed with 100 mL of double distilled water (DDW) in a 250 mL beaker, and then heated to boil for 10 min. The resulting aqueous plant solutions were filtered with qualitative filter paper disks (Munktell, grade 388). Finally, the filtrates of the aqueous plant extracts were stored in the dark at 4 °C until use.

2.2. Biosynthesis of AuNPs with plant aqueous extracts

For the biosynthesis of AuNPs, 10.0 mL of 1% (v/v) filtered plant extracts (*M. piperita*, *S. officinalis*, or *M. officinalis*) in DDW were directly mixed with either 2.5, 1.1, or 0.53 mL of a 1000 mg L⁻¹ Au(III) stock solution to produce final Au(III) concentrations of 200, 100, or 50 mg L⁻¹, respectively. The stock solution of Au(III) was obtained by dissolving an appropriate amount of HAuCl₄ × 4H₂O (Avantor Performance Materials, Gliwice, Poland) in DDW. The influence of the temperature of the reaction mixtures and the concentration of Au(III) on the size of the biosynthesized AuNPs and their size distribution were investigated by mixing the pre-warmed aqueous plant extracts with solutions of Au(III). Then, the reaction mixtures were incubated for 24 h at 20, 40, or 60 °C in a water bath. To monitor the influence of the incubation time, samples containing the produced AuNPs were taken following 0.167, 0.333, and 24 h of incubation and subjected to measurements by UV-Vis absorption spectrophotometry.

2.3. The design and operation of the dc-μAPGD system

To examine any potential interaction effects of dc-μAPGD with plant extract mediated reduction, the AuNPs biosynthesized with the plant aqueous extracts were treated by dc-μAPGD in a miniature reactor. This discharge system consisted of an Ar nozzle microjet as the anode and a flowing liquid cathode (Fig. 1). The solution of the flowing liquid cathode consisted of the products of the 1% (m/v) plant extract and 50 mg L⁻¹ Au(III) ions following the 24 h incubation at 20 °C. The microdischarge was ignited by a Pt wire in the gap between electrodes, and was sustained by applying a voltage of 1300 V to both electrodes. This resulted in a current flow of 45 mA. The flow rate of the solutions of the flowing liquid cathode was 3 mL min⁻¹, and the flow rate of the Ar nozzle microjet-supporting gas was 120 sccm. Following the passage of the reaction mixtures through the miniature reactor, the product was collected in small vials for further analysis.

2.4. Characterization of AuNPs

2.4.1. UV-Vis absorption spectrophotometry

The bioreduction of the Au(III) ions to Au⁰ was monitored by UV-Vis absorption spectrophotometry using a Specord 210

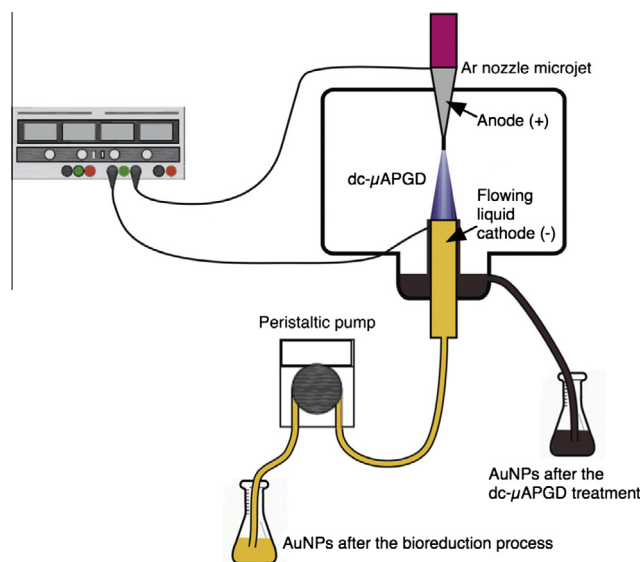


Figure 1 Schematic of the dc-μAPGD system used in this study. The setup of the dc-μAPGD system is shown, and the relevant aspects are labeled.

Plus (Analytik Jena, Jena, Germany) instrument. The absorption spectra were acquired in the range of 400–1100 nm with a step of 0.1 nm and a scanning speed of 20 nm s⁻¹. The measurements were carried out ~10 min after the bioreduction process was completed. The UV-Vis absorption spectrum of DDW was used as the background reference. Additionally, the UV-Vis absorption spectra of the aqueous plant extracts were collected and compared with the spectra obtained for the solutions containing the biosynthesized AuNPs. To monitor the formation of AuNPs over the time, the absorbance at a wavelength of 530 nm (the position of the localized surface plasmon resonance [LSPR] band) was measured every 0.2 s for 180 s, with an integration time of 0.04 s.

2.4.2. Dynamic light scattering

For the determination of the size of the obtained AuNPs, they were purified by centrifugation at 12,000 rpm for 10 min in a MPW-350 centrifuge (MPW Medical Instruments, Warsaw, Poland). The size by volume of the AuNPs was determined by dynamic light scattering (DLS), using a Nicomp 380ZLS (Particle Sizing Systems, Port Richey, FL, USA) particle sizing system equipped with a green laser excitation source operating at 532 nm/50 mW. A frequency of the photon counting was set at 200 kHz, while a scattering angle was fixed at 90°. The temperature of the measured media was within 24–27 °C. Disposable poly(methyl methacrylate) (PMMA) square cuvettes (ID of 1.0 cm) were used. The hydrodynamic diameter of the AuNPs was calculated based on the Stokes-Einstein equation (Huang et al., 2014), considering water as a continuous phase (the water viscosity was within 0.911–0.852 mPa s, and the diffusion coefficient of NPs was within 6.89 × 10⁻⁹–5.30 × 10⁻⁸ cm² s⁻¹). A Nicomp CONTIN mode was used for analysis, and up to three modes could be calculated; volume weighting has been used for work-up of results.

2.4.3. Scanning electron microscopy

Scanning electron microscopy (SEM) was used to confirm the production of AuNPs and examine the morphology of the

obtained AuNPs. SEM images were acquired using a JSM-6610LVnx (Jeol, Tokyo, Japan) instrument that was equipped with an Aztec Energy (UK) integrated X-ray energy dispersive spectrometer (EDS) and a high-resolution CCD camera. The solutions with the purified AuNPs were dispersed in DDW using a vortex and placed on a carbon sticky conductive tape, and the solutions allowed to be evaporated. SEM images were recorded at magnifications from 15,000 \times to 18,000 \times . An accelerating voltage of 20–25 kV was applied.

2.4.4. Transmission electron microscopy and X-ray energy dispersive spectrometry

The size, the particle shape distribution, and the elemental composition of the AuNPs were acquired by transmission electron microscopy (TEM) and energy dispersive spectrometry (EDS) using a FEI Tecnai G²20 X-TWIN instrument (FEI, Hillsboro, Oregon, USA) supported with an EDAX X-ray microanalyzer (FEI). For this purpose, one drop of the Au suspensions was put on a Cu mesh grid and allowed to dry. Due to the high resolution of TEM, it was not necessary to purify the AuNPs before measurements by centrifugation. The AuNPs size was determined by calculating the diameter of the spherical NPs, the height of the triangular NPs, the length of nanorods, and the diameter of nanostars, and was based on 60 measurements.

2.5. Qualitative and quantitative composition of the aqueous plant extracts

2.5.1. Attenuated total reflection Fourier transform infrared (ATR-FTIR) spectroscopy

The qualitative composition of the leaf extracts of *M. piperita*, *S. officinalis*, and *M. officinalis*, both with and without HAuCl₄ and in reference to the presence of different classes of the organic compounds was assessed using ATR-FTIR. The ATR-FTIR spectra were acquired using a Vertex 70v (Bruker, Germany) Fourier transform infrared spectrometer equipped with a diamond ATR cell. The absorption spectra were measured at room temperature in the range of 4000–400 cm⁻¹ for the pure aqueous plant extracts as well as for the post-reaction mixtures, i.e., after the addition of the solutions of HAuCl₄.

2.5.2. Folin–Ciocalteu assay

The total concentration of the phenolic compounds in the aqueous plant extracts, as well as the post-reaction mixtures, was determined with UV–Vis absorption spectrophotometry using the Folin–Ciocalteu (F–C) assay (Stratil et al., 2006). In this assay, 2.5 mL of a F–C reagent solution (Sigma-Aldrich, Poznan, Poland), which contained a mixture of phosphomolybdate and phosphotungstate (3H₂O \times P₂O₅ \times 14WO₃ \times 4MoO₃ \times 10H₂O), was added to 0.5 mL of the solutions of each plant leaf extract. The mixtures were incubated for 2 min at room temperature, following which 2.0 mL of a 7.5% (m/v) Na₂CO₃ solution was added. The resulting mixtures were subsequently incubated for 15 min at 50 °C and finally cooled in a water–ice bath for 4 min. The absorbance of the solutions at 734 nm was immediately measured. Gallic acid (GA) was used as a standard, and the calibration solutions contained from 30 to 150 mg L⁻¹ of GA. The final results are expressed as GA equivalents.

3. Results

3.1. All three aqueous plant extracts can successfully be employed in AuNP biosynthesis

To initially test whether the aqueous plant extracts were capable of synthesizing the AuNPs, HAuCl₄ \times 4H₂O solutions (1000 mg L⁻¹ of Au) were added to freshly prepared 1.0% (m/v) aqueous plant extracts (*M. piperita*, *S. officinalis*, or *M. officinalis*) to a final concentration of 200 mg L⁻¹, and the mixtures were incubated at 20 °C for 24 h. Following incubation, a color change of the post-reaction mixtures from dark yellow into ruby red and bluish was observed. Such a color shift was observed for the aqueous extracts of all studied plants and was indicative of the biosynthesis of AuNPs (Dzimitrowicz et al., 2015a; Bhambure et al., 2009). This confirmed that the extracts of all three studied plants could successfully reduce the Au(III) ions to Au⁰. The color change was likely a consequence of the appearance of the LSPR absorption band for the biosynthesized AuNPs, which has a characteristic maximum in the range within 520–580 nm (Pal and Kryschi, 2015).

To confirm the visual observations, UV–Vis absorption spectrophotometry was used to measure the position of the maximum of the LSPR band. Representative absorption spectra for the AuNPs synthesized from each extract are shown in Fig. 2. A LSPR band between 520 and 580 nm was observed in each spectra, which further supports the production of AuNPs. A wide plasmonic band was detected in the samples synthesized from the *M. piperita* aqueous leaf extract, which indicated the production of the uniform and spherical AuNPs. In contrast, two bands were seen in each of the samples synthesized by the *S. officinalis* or *M. officinalis* extracts; a LSPR band for the spherical AuNPs and a longitudinal plasmon resonance band indicative of the nanostructures of different shapes, e.g. triangles, rods, or stars.

The AuNPs samples were examined with SEM to confirm the presence of AuNPs. As shown in Fig. 3, the non-aggregated grains of AuNPs were synthesized regardless of which aqueous leaf extract was used. However, due to the limited resolution of SEM, no clear differences in the size or shape of the obtained AuNPs could be observed. For this purpose, TEM was used. Under the given conditions (200 mg L⁻¹ Au (III) and 20 °C), the smallest AuNPs were formed using the *S. officinalis* extract (Fig. 4). Their average size was 15.1 \pm 10.2 nm, and they were mostly spherical (52%) or triangular (27%), although different shapes such as stars (16%), and rods (5%) were also observed for them. A variety of particle shapes were also noticed for the AuNPs synthesized with the *M. officinalis* extract (Fig. 5). The AuNPs had an average size of 19.5 \pm 24.3 nm, with spherical (60%), triangular (23%), star shaped (13%), and rod shaped (3%) structures seen. When the *M. piperita* extract was used for the AuNPs synthesis, the AuNPs were primarily spherical and had a higher average size and size distribution, i.e. 55.1 \pm 48.4 nm (Fig. 6), than those obtained in the other cases.

The EDS measurements were performed to examine the elemental composition of the nanoparticles and their surrounding (Fig. 7). The results unambiguously confirmed the presence of metallic Au. In all aqueous leaf extracts there were found small amounts of C, Cl, K, and Ca. These elements

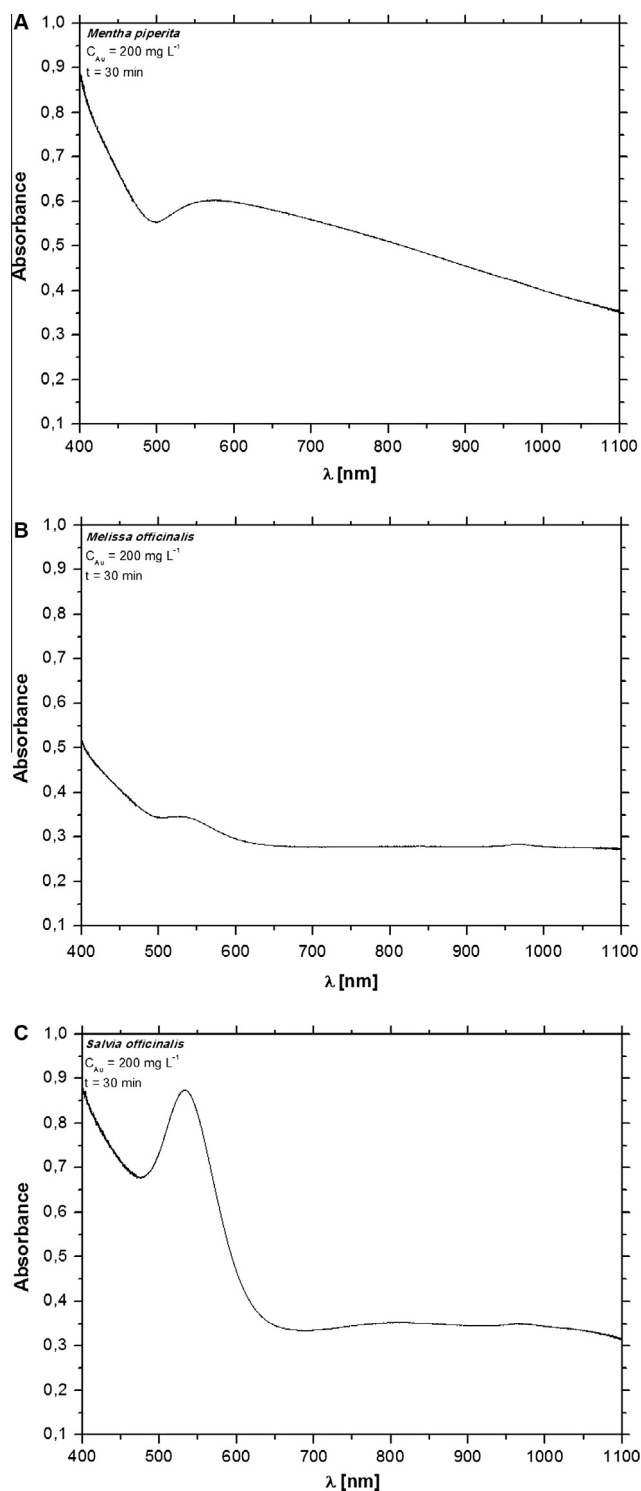


Figure 2 UV-Vis spectra of AuNPs produced at 20 °C and 200 mg L⁻¹ using the aqueous plant extracts. Spectra are shown for AuNPs synthesized using either (a) *M. piperita*, (b) *M. officinalis*, or (c) *S. officinalis*.

were present due to the elemental composition of the extracts, from which the AuNPs were not purified prior to EDS analysis. The presence of Cu is due to the Cu grid, on which the samples were analyzed. Thus, all measurement techniques

confirmed that the aqueous leaf extracts of *M. piperita*, *S. officinalis*, and *M. officinalis* can be effectively used in the biosynthesis of the AuNPs.

3.2. Effects of reaction parameters on the size of the produced AuNPs

To determine the optimal conditions for the biosynthesis of the AuNPs using the aqueous plant extracts, the effect of the reaction temperature, the length of incubation, and the concentration of Au(III) ions were examined in reference to the position of the maximum of the LSPR absorption band. According to the Mie scattering theory, the size of NPs is correlated with the extent of the red-shift of the LSPR absorption band (Hao and Schatz, 2004). Using 200 mg L⁻¹ solutions of the Au(III) ions and incubating them with each of the aqueous plant extracts at 20 °C, the position of the maximum of the LSPR absorption band was determined using UV-Vis absorption spectrophotometry following 0.166, 0.333 and 24 h of the incubation (Table 1). For all three plant extracts used, the position of the maximum of the LSPR absorption band remained fairly constant over the time, and no correlation between the time and the position of the maximum of the LSPR band was found. Thus, AuNPs with the ultimate size were obtained within the first 10 min of the reaction.

To examine the influence of the type of the plant taken for preparing the extract on the kinetics of the AuNPs biosynthesis, the rate of the AuNPs biosynthesis was further studied by using UV-Vis absorption spectrophotometry (Fig. 8). The maximal rate of the AuNPs bio-synthesis for both aqueous *M. piperita* and *M. officinalis* extracts was similar, i.e., 0.19 and 0.18 ΔA₅₃₀ s⁻¹, respectively, while that of the *S. officinalis* extract was slower, i.e., 0.07 ΔA₅₃₀ s⁻¹. Nevertheless, regardless of the aqueous plant extract used, the AuNPs biosynthesis was completed within 1 min of the incubation.

In addition, it was found that all three plant extracts could successfully be employed in the synthesis of AuNPs regardless of the concentration of the Au(III) ions (50, 100, 200 mg L⁻¹) or the incubation temperature (20, 40 and 60 °C), as in all cases a shift in color of the post-reaction mixtures from yellow to ruby red/bluish was observed. However, the intensity of the mentioned ruby red/bluish color was established to increase with the concentration of the AuNPs precursor. DLS was used to examine how these different reaction parameters influenced the size of the obtained AuNPs. The effect on the size by volume of AuNPs in response to changes in the concentration of the Au(III) ions and the incubation temperature was unique for each of the aqueous plant extracts examined (Fig. 9a-c). Nevertheless, the best conditions to obtain AuNPs with the smallest size for the aqueous extracts of both *M. piperita* and *M. officinalis* were a low incubation temperature (20 °C) and a low concentration of Au (50 mg L⁻¹). In the case of the aqueous extract of *S. officinalis*, the best conditions for the production of the smallest in size AuNPs were slightly different, requiring a moderate incubation temperature (40 °C) and a medium concentration of Au (100 mg L⁻¹). By comparing the size of the AuNPs biosynthesized at the established optimal conditions (Fig. 9d), it was found that *M. piperita* was by far the best plant for facilitating the production of AuNPs, with an average size that was 32.2% and 16.9% of the size of the AuNPs produced with the aid of *M. officinalis* and *S. officinalis*, respectively.

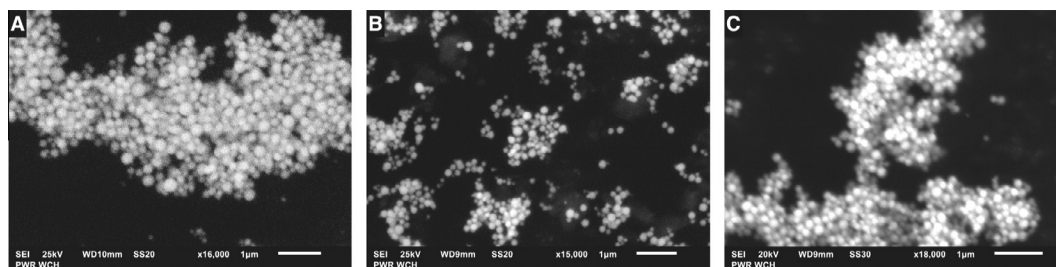


Figure 3 The SEM micrographs of the AuNPs obtained using the aqueous plant extracts. AuNPs were obtained following the 24 h incubation at 20 °C of the 200 mg L⁻¹ Au(III) solutions with the aqueous extracts of (a) *M. piperita*, (b) *M. officinalis*, or (c) *S. officinalis*.

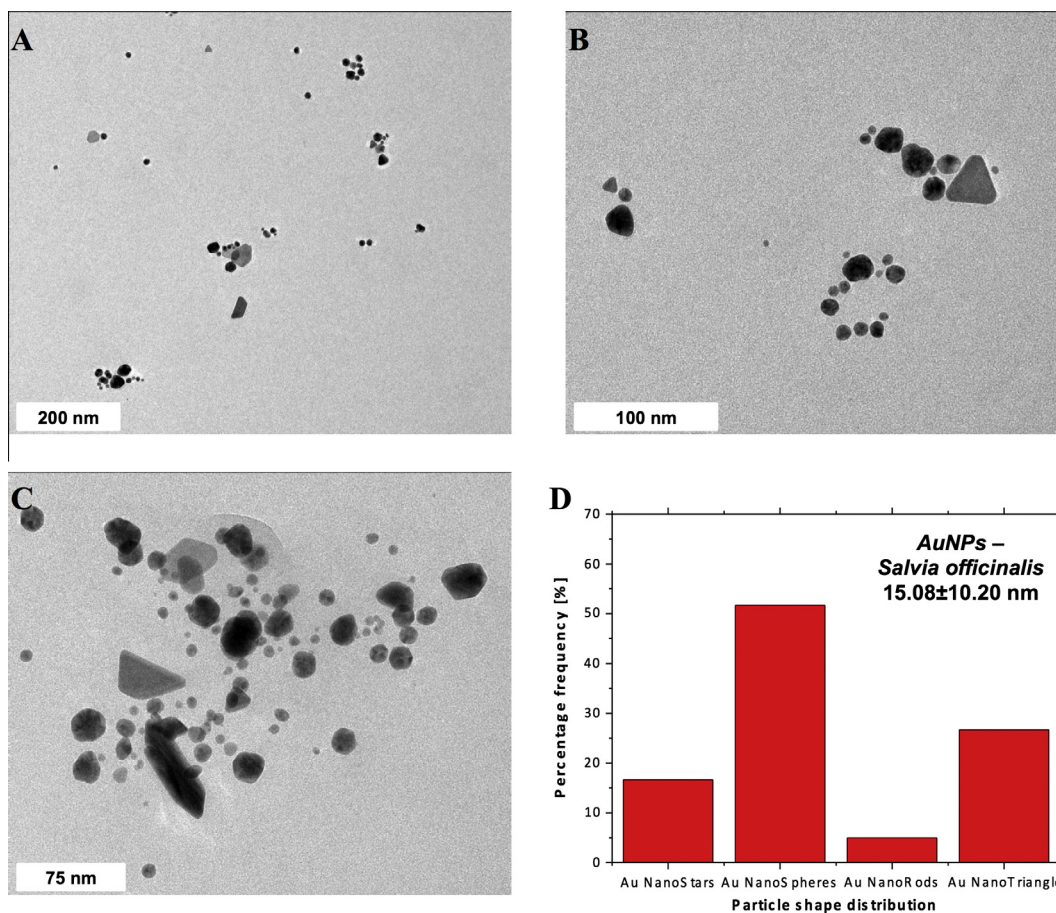


Figure 4 TEM micrographs illustrating the size and morphology of AuNPs obtained with the *S. officinalis* extract. (a–c) Representative TEM micrographs of the AuNPs produced using 200 mg L⁻¹ Au(III) at 20 °C are shown. (d) The size and shape distribution of the AuNPs is presented.

3.3. Examination of the bioactive compounds in the aqueous plant extracts

In order to gain some understanding of the active organic compounds present in the aqueous plant extracts that were involved in facilitating the biosynthesis of AuNPs, these extracts were measured by ATR-FTIR before and after the incubation with the Au(III) ions (Fig. 10). The absorption bands associated with the compounds involved in the Au(III) reduction or stabilization of the AuNPs were expected to be shifted following the addition of the Au(III) ions (Elia

et al., 2014). Indeed, the shifts in the multiple bands were observed following the incubation of the aqueous plant extracts with the solutions of the Au(III) ions (Table 2). For the aqueous leaf extracts of all three plants, the shifts in the position of the bands were associated with the hydroxyl groups of the phenolic compounds, secondary amines, and either nitriles, aliphatic amines, or phenols. However, as the exact position of these bands in each of the aqueous plant extracts differed, it is likely that the specific compounds involved in the biosynthesis of AuNPs in each extract were different.

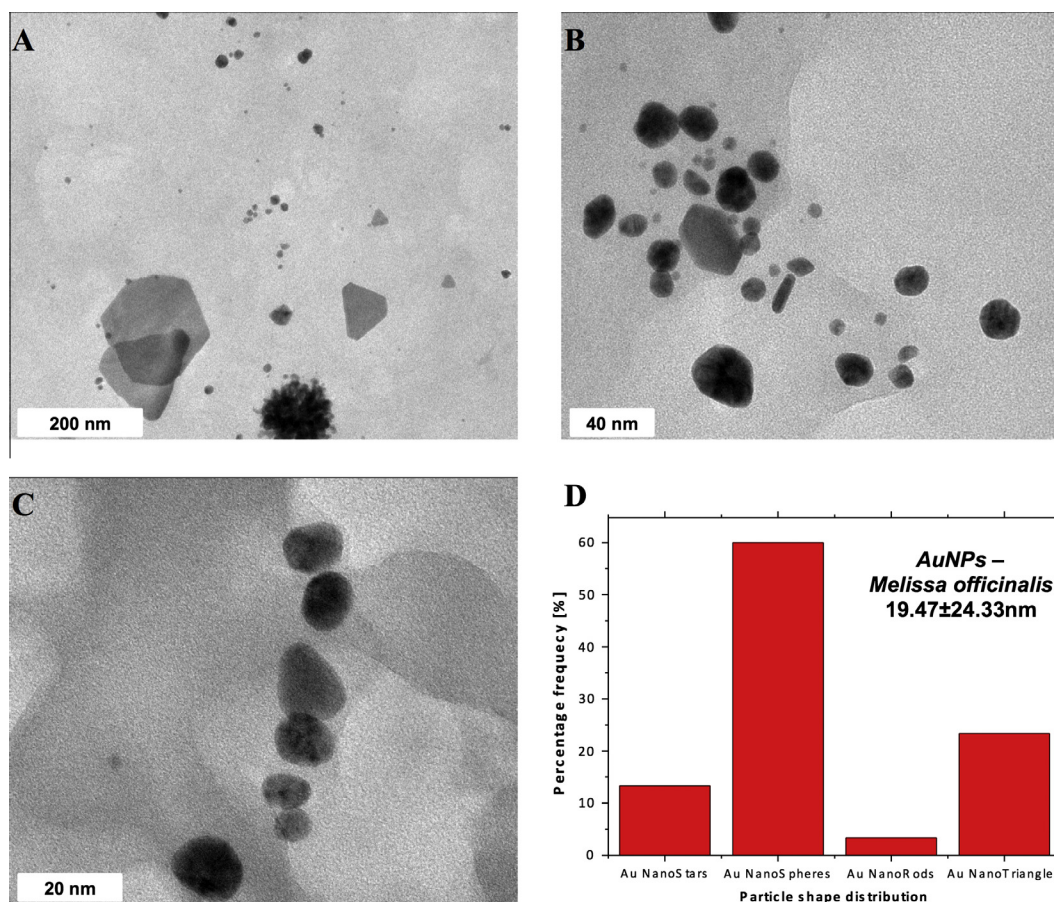


Figure 5 TEM micrographs illustrating the size and morphology of AuNPs obtained with the *M. officinalis* extract. (a–c) Representative TEM micrographs of the AuNPs produced using 200 mg L^{-1} Au(III) at 20°C are shown. (d) The size and shape distribution of the AuNPs is presented.

3.4. The role of the phenolic compounds in the biosynthesis of AuNPs

In the ATR-FTIR spectra of the aqueous extracts of all three plants, two bands potentially related to phenolics were observed to undergo the highest shifts following the addition of the HAuCl_4 solutions (Table 2). Therefore, the potential role of the phenolic compounds in the biosynthesis of AuNPs by the aqueous extracts of *M. piperita*, *M. officinalis*, and *S. officinalis* was further examined by measuring the total concentrations of these organic species in the aqueous plant extracts before and after incubation with the added solutions of HAuCl_4 (Table 3). It was established that there was an inverse relationship between the concentration of phenolics and the amount of the added AuNPs precursor. This pointed out that the reduction of the Au(III) ions to Au^0 was associated with the oxidation of the plant derived phenolics. An inverse correlation was also found between the initial concentration of phenolics and the size of AuNPs biosynthesized at conditions providing the smallest NPs (Fig. 9). Furthermore, it was noted that the aqueous extract of *S. officinalis* had the lowest concentration of the phenolic compounds as well as the slowest rate of the AuNPs biosynthesis (Table 3 and Fig. 8). Hence, it was concluded that phenolics play a very important role in the reduction and stabilization of the Au

(III) ions to Au^0 during the biosynthesis of AuNPs by the natural plant extracts.

3.5. The dc- μ APGD treatment of the biosynthesized AuNPs

While APP has previously been used to generate spherical AuNPs (Dzimitrowicz et al., 2015a,b), the effect of treating the previously obtained AuNPs with the plasma has not been studied so far. Therefore, it was examined whether the dc- μ APGD treatment of the biosynthesized AuNPs could improve their quality. To accomplish this, AuNPs were biosynthesized using each of the three aqueous plant extracts and 50 mg L^{-1} of Au(III) ions. The post-reaction mixtures containing the colloidal AuNPs were passed through the dc- μ APGD based reactor, and the size of the AuNPs in the collected solution was determined with DLS 24 h after the dc- μ APGD treatment (Fig. 9e). In fact, the plasma treatment resulted in an enlargement of the size of the biosynthesized AuNPs by at least 3-fold.

4. Discussion

In recent years, the use of the plant extracts in the synthesis of various types of nanoparticles has been examined, and many

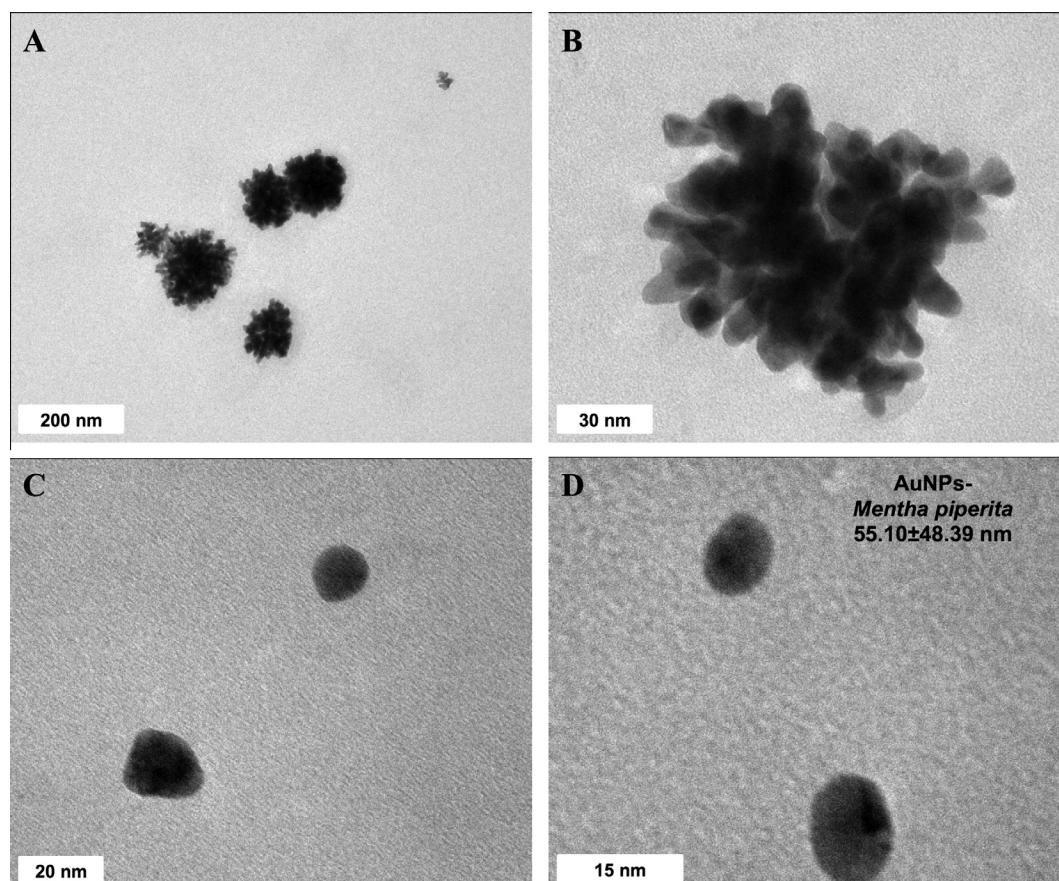


Figure 6 TEM micrographs illustrating the size and morphology of AuNPs obtained with the *M. piperita* extract. (a–c) Representative TEM micrographs of the AuNPs produced using 200 mg L^{-1} Au(III) at 20°C are shown. (d) The size distribution is indicated. As the AuNPs were primarily spherical, a shape distribution was not determined.

of these studies are nicely summarized in recent review articles (Singh et al., 2016; Hussain et al., 2016). Extracts from numerous plants were employed for the biosynthesis of AuNPs, and the sizes of the obtained AuNPs are listed in Table 4. As can be seen, while most of the studies report the sizes between 10 and 50 nm, sizes as large as 300 nm have been also reported (Table 4). It can be seen that even with the same plant used for the preparation of the extract, the AuNPs of different sizes can be produced (Table 4). The sizes of the AuNPs obtained in this study fell within the range of the values reported in the literature.

A disadvantage of comparing the results between studies is that it is difficult to attribute differences to the plant material, as the differences could also be due to the varying methods of the extract production and the AuNPs synthesis reaction conditions. This prompted us to examine the properties of the *M. piperita*, *M. officinalis*, and *S. officinalis* extracts using the standardized methods and a common set of the reaction parameters. The effect of the plant material, the incubation temperature, the Au(III) ions concentration, and the incubation length on the size of the obtained AuNPs were examined. However, it was not examined how different preparation methods may influence the properties of the extract. Like in many other groups (Khalil et al., 2012; Suman et al., 2014; Singh et al., 2015; Klekotko et al., 2015; Dhamecha et al., 2016, among others), the extracts were prepared by boiling the

ground plant material in distilled water, while others have prepared the extracts with heating to lower temperatures (MubarakAli et al., 2011), at room temperature (Elia et al., 2014), with microwave irradiation (Yallappa et al., 2015a; Patra et al., 2015), or with methanol extraction (Kumar et al., 2011). Given that many organic compounds are heat labile, it was expected that the extracts produced at different temperatures would have different properties.

The DLS data presented here illustrated that, at least under the examined conditions, the *M. piperita* extract facilitated the production of the AuNPs at least 16% smaller than those obtained using the extracts of *M. officinalis* and *S. officinalis* (Fig. 9). When the AuNPs were synthesized under the originally tested conditions (200 mg L^{-1} and 20°C), the AuNPs produced by the *M. piperita* extract were larger and agglomerated (Fig. 6), unlike those produced by using the extracts of *M. officinalis* or *S. officinalis* (Figs. 4 and 5). This is consistent with the large size prediction based on the DLS data with these conditions (Fig. 9). However, it was expected that the AuNPs produced by the *M. piperita* extract under the optimal conditions (50 mg L^{-1} and 20°C) were not agglomerated; otherwise, DLS would have indicated much larger sizes for the obtained AuNPs. It was also noted that the observed sizes of the obtained AuNPs appeared larger when measured using DLS as compared to the size measured with TEM, and that it is commonly accepted that DLS overestimates the NP sizes.

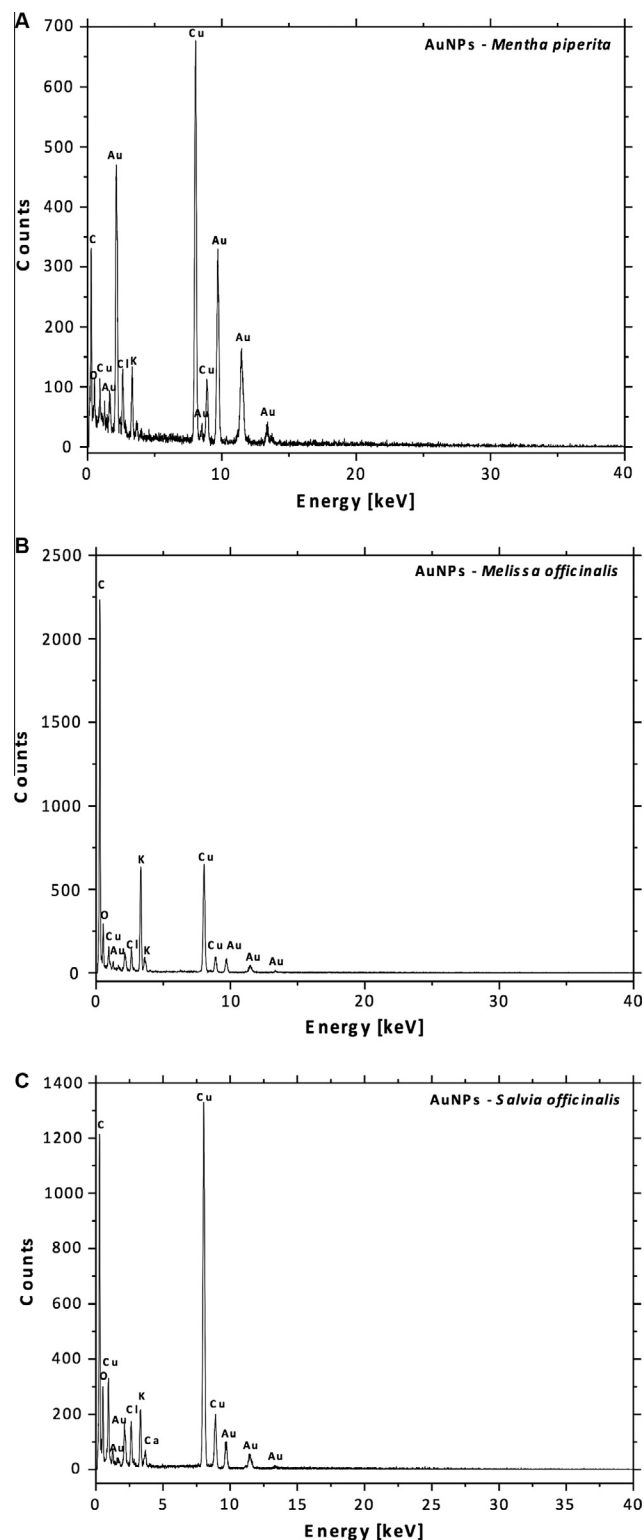


Figure 7 EDS spectra of the AuNPs produced using the aqueous plant extracts. EDS spectra for AuNPs produced with (a) *M. piperita*, (b) *M. officinalis*, or (c) *S. officinalis* are shown. In all cases, peaks are labeled. Gold is detected in all, consistent with the formation of AuNPs, while the other elements are due to trace elements in the extracts and the use of a copper grid for sample analysis.

Table 1 The position (in nm) of the maximum of the LSPR absorption band following the biosynthesis of AuNPs.

Aqueous leaf extract	Time (h)		
	0.167	0.333	24
<i>M. piperita</i>	580.6	577.0	577.5
<i>M. officinalis</i>	524.8	526.9	525.2
<i>S. officinalis</i>	531.7	531.2	524.6

Reactions were performed at 20 °C using the 200 mg L⁻¹ solutions of Au(III).

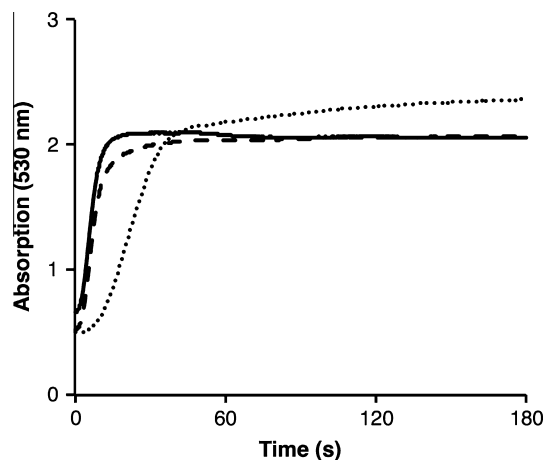


Figure 8 The kinetics of the AuNPs biosynthesis using the aqueous plant extracts. The AuNPs biosynthesis was carried out at 20 °C using the 200 mg L⁻¹ Au(III) solutions and the aqueous extracts of *M. piperita* (solid line), *M. officinalis* (dashed line) and *S. officinalis* (dotted line).

Monitoring the rate of the AuNPs production at 530 nm illustrated that the maximal yield was largely obtained within the first minute of incubation regardless of the plant source (Fig. 8), although a slight yield increase continued to be observed for the *S. officinalis* extract until the three minute mark. In comparison, other have reported that the AuNPs synthesis times were required under 10 min of incubation with plant aqueous extracts (Kumar et al., 2011; Singh et al., 2015, 2016), with Song et al. (2009) reporting 79% conversion within the first minute. In contrast, traditional chemical reduction procedures are much longer, multi-step processes (Kumar et al., 2011; Singh et al., 2016). Thus, the method reported here allows for the rapid synthesis of the AuNPs. Additionally, based on the maximal LSPR band absorbance at 530 nm, the yield of the AuNPs was similar regardless of the plant extract used (Fig. 8). Considering both the change in absorbance from the start to end of the reaction and the concentration of the precursor Au(III) ions, the yield obtained through the procedure described here is similar to or better than that reported in many other studies using the plant extracts (such as Dhamecha et al., 2016; Yallappa et al., 2015a; Suman et al., 2014). The yield is not as high, however, as that obtained with the method of Jia et al. (2012) based on

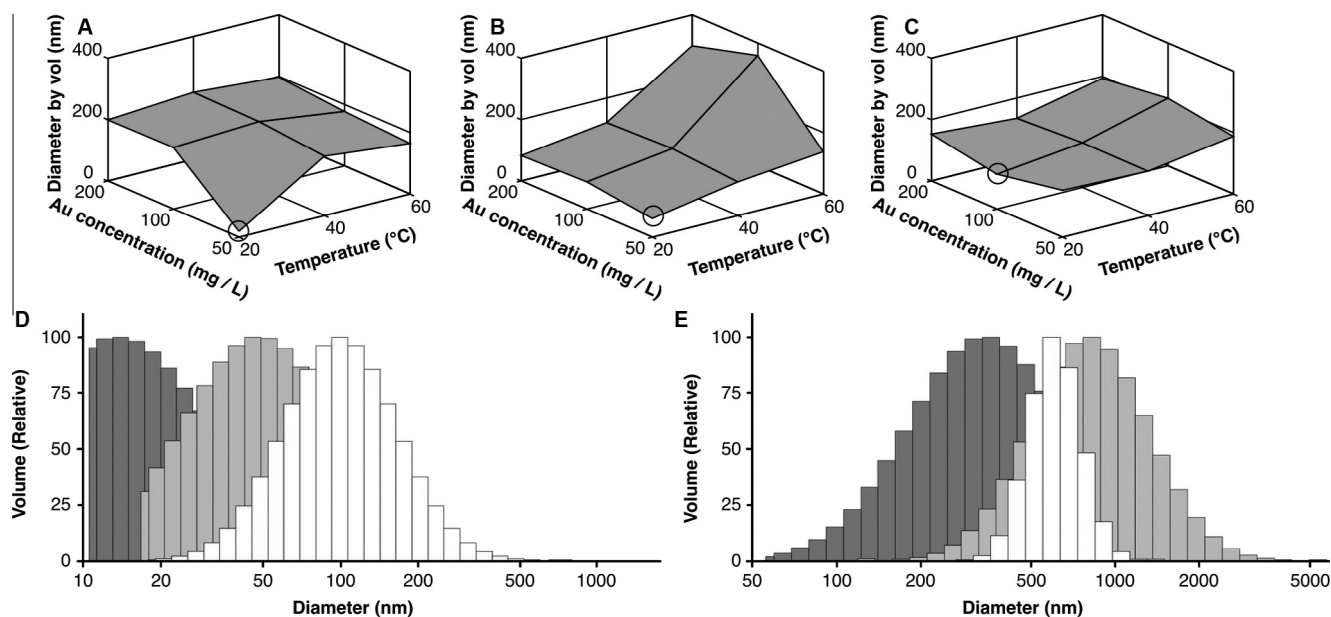


Figure 9 The effect of the type of the aqueous plant extract, the reaction conditions, and the plasma treatment on the size of the obtained AuNPs. The effect of the concentration of Au and the incubation temperature on the size of the obtained AuNPs, as determined by DLS, following the 24 h incubation of the solutions of Au with the aqueous leaf extracts of (a) *M. piperita*, (b) *M. officinalis*, or (c) *S. officinalis*. The best reaction conditions are indicated by the squares. (d–e) The size distribution of the AuNPs obtained under the optimal reaction conditions for the aqueous leaf extracts of *M. piperita* (dark gray), *M. officinalis* (light gray), and *S. officinalis* (white). The size distribution of the AuNPs obtained in the 50 mg L⁻¹ Au(III) solutions following the 24 h incubation at 20 °C with the aqueous leaf extracts of *M. piperita* (dark gray), *M. officinalis* (light gray), and *S. officinalis* (white) (d) before and (e) after the plasma treatment.

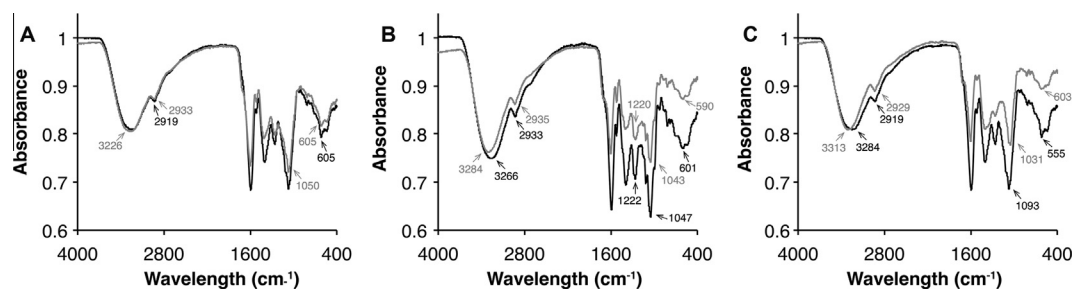


Figure 10 ATR-FITR spectra of the aqueous extracts. Spectra are shown for the (a) *M. piperita*, (b) *M. officinalis*, or (c) *S. officinalis* extracts before (black line) and after (gray line) the addition of Au(III) to a final concentration of 200 mg L⁻¹.

Table 2 Shifts of the ATR-FTIR spectra bands after the addition of the aqueous plant extracts to the HAuCl₄ solutions.

Organic compound	Aqueous extract					
	<i>M. piperita</i>		<i>M. officinalis</i>		<i>S. officinalis</i>	
	Without Au	With Au	Without Au	With Au	Without Au	With Au
Alcohol, phenol	3220	3226	3266	3284	3284	3313
Nitrile, aliphatic amines, phenols	1047	1050	1047	1043	1093	1031
Secondary amines	2919	2933	2933	2935	2919	2929
Amine III and amine I	ND ^a	ND ^a	1222	1224	ND ^a	ND ^a
C–Cl	605	605	601	590	555	603

^a ND, Corresponding bonds not detected.

isolated ethoxylated polyester that can be purified from a plant material. Taken together, all of these data reported here support that the use of the *M. piperita* extracts is a promising

alternative to the use of the toxic chemical reductants in the production of the AuNPs on an enlarged and semi-industrial scale.

Table 3 Concentration of polyphenols (mg per 100 gGA) in the aqueous plant extracts before and after the addition of the HAuCl₄ solutions.

Concentration of Au (mg L ⁻¹)	Aqueous extract		
	<i>M. piperita</i>	<i>M. officinalis</i>	<i>S. officinalis</i>
0	57.62	86.67	36.45
50	55.56	81.86	34.30
100	53.69	76.21	21.49
200	51.63	74.47	19.92

Despite the increasing attention being given to the synthesis of the AuNPs with natural plant extracts, the bioreduction mechanism remains to be elucidated (Singh et al., 2016). Other studies have suggested that a variety of molecules may play a role, including proteins and metabolites, and that the mechanism may even be plant specific (Baker et al., 2013; Duan et al., 2015; Singh et al., 2016). Consistent with this, the ATR-FTIR data reported here (Fig. 10) were consistent with the involvement of the multiple compounds in the AuNPs synthesis. Additionally, as the specific location of bands differed between the plants, different molecules belonging to the same chemical families likely participated in the AuNPs synthesis in the different extracts.

Two of the strongest shifts in the ATF-FTIR spectra following the addition of the Au(III) ions appeared to be associated with polyphenols. Polyphenols have previously been suggested to be involved in the plant extract mediated AuNPs synthesis on the bases of the FTIR data (Song et al., 2009; Khalil et al., 2012; El-Kassass and El-Sheekh, 2014; Murugan et al., 2015); however, this had not been conclusively demonstrated. This claim is supported by work of Huang et al. (2010) showing that purified polyphenols can be used to synthesize the AuNPs, although that study did not address the *in vivo* role of polyphenols in crude plant extracts. Therefore, the F-C assay was employed in an attempt to gather a more direct evidence for the involvement of polyphenols. The decrease in the concentration of polyphenols with increasing concentrations of the AuNPs precursor (Table 3) provides the strong and more direct evidence that polyphenols are oxidized during the reduction of the Au(III) ions. A decrease in the phenolic content in the *Nepenthes khasiana* extracts following the formation of AuNPs was also very recently observed (Dhamecha et al., 2016). The role of phenolics was further supported by the observed relationships between their concentration and the size and synthesis rate of AuNPs. However, the differential effects of the incubation temperature and the concentration of the Au(III) ions on the size of the AuNPs produced with each of the aqueous plant extracts cannot be simply explained by the content of the phenolics. Hence, the type of the phenolics, as well as the type of other compounds present in the plant extracts, is likely to influence both the size of the obtained AuNPs and the response of the size to the changing reaction conditions.

In addition to plant extracts, lasers (e.g. Kuladeep et al., 2012; Maximova et al., 2015) and APPs (Hieda et al., 2008; Shirai et al., 2014; Dzimitrowicz et al., 2015a,b) can be employed in the green synthesis of AuNPs. Past work has illustrated that lasers can be used to synthesize AuNPs from

Table 4 A partial list of the sizes of AuNPs synthesized by plant aqueous extracts reported in the literature.

Plant	Measurement method	Size (nm)	References
<i>Acalypha indica</i>	TEM	20–30	Krishnaraj et al. (2014)
<i>Anethum graveolens</i>	TEM	10	Fierascu et al. (2010)
<i>Butea monosperma</i>	TEM	10–30	Patra et al. (2015)
<i>Cassia auriculata</i>	TEM	15–25	Kumar et al. (2011)
<i>Corallina of cinalis</i>	TEM	14.6	El-Kassass and El-Sheekh (2014)
<i>Cymbopogon citratus</i>	TEM	20–50	Murugan et al. (2015)
<i>Jasminum sambac</i>	FE-SEM/TEM	20–50	Yallappa et al. (2015a)
<i>Lippia citriodora</i>	SEM	36	Elia et al. (2014)
<i>Mappia foetida</i>	FE-SEM/TEM	10–20	Yallappa et al. (2015b)
<i>Melissa officinalis</i>	TEM	20	This study
<i>Mentha piperita</i>	SEM	150	MubarakAli et al. (2011)
<i>Mentha piperita</i>	TEM	55	This study
<i>Mentha piperita</i>	DLS	19	This study
<i>Morinda citrifolia</i>	TEM	12–39	Suman et al. (2014)
<i>Nepenthes khasiana</i>	DLS	125–180	Dhamecha et al. (2016)
<i>Olea europaea</i>	TEM	50–100	Khalil et al. (2012)
<i>Panax ginseng</i>	FE-TEM	10–20	Singh et al. (2015)
<i>Pelargonium graveolens</i>	SEM	45	Elia et al. (2014)
<i>Punica granatum</i>	SEM	32	Elia et al. (2014)
<i>Salvia officinalis</i>	SEM	29	Elia et al. (2014)
<i>Salvia officinalis</i>	TEM	15	This study
<i>Syzygium jambolanum</i>	HRTEM	20–30	Karthick et al. (2015)
<i>Zingiber officinale</i>	TEM	10	Singh et al. (2011)

the Au(III) ions (Kuladeep et al., 2012), as well as to fragment the existing AuNPs to produce the AuNPs of smaller sizes (Maximova et al., 2015). It has been recently demonstrated in our group that AuNPs can be synthesized from the Au(III) ions by dc-μAPGD in a flowing liquid solution (Dzimitrowicz et al., 2015a,b), but had not previously examined whether this system could also serve to split the existing AuNPs. Here, it was observed that the passage of the AuNPs synthesized by the natural plant extracts did not reduce their size, but instead resulted in an enlargement. There are two possible explanations for that. The dc-μAPGD treatment resulted in the partial evaporation of the water in these solutions, increasing the concentration of the AuNPs, potentially leading to their agglomeration. Alternatively, it may be

that the plasma treatment, either the plasma itself or the heat generated during the dc- μ APGD treatment, disrupted stabilizing the interactions between the AuNPs and the natural compounds in the extracts. This would therefore provide new opportunities for the chemical reactions, leading to aggregation and sedimentation of the AuNPs.

5. Conclusions

By examining the AuNP synthesis properties of the aqueous extracts of three evolutionarily related plant species under standardized conditions, it is possible to directly compare them and observe that the optimal reaction conditions differed for each. Under optimal conditions, the *M. piperita* extract produced the small sized AuNPs. The use of the F–C assay provided clear evidence implicating phenolics in the reduction of the Au(III) ions and the production of AuNPs. Finally, treatment of the biosynthesized AuNPs with the aqueous plant extracts with dc- μ APGD resulted in an enlargement of the NPs.

Authors' contributions

AD, GD, PJ and PP conceived and designed all experiments, and analyzed and summarized the obtained results. AD and PJ carried out measurements by UV–Vis absorption spectrophotometry. AD performed all measurements by ATR–FTIR in addition to the F–C assay. AD purified the synthesized AuNPs. AD, IS and TK carried out measurements by DLS. AD and GD prepared the manuscript. PJ and PP supervised the work and reviewed the manuscript. All authors read and approved the final manuscript version.

Acknowledgments

This work was financed by a statutory activity subsidy from the Polish Ministry of Science and Higher Education for the Faculty of Chemistry of Wrocław University of Technology. In addition, support from the Wrocław Centre of Biotechnology, program The Leading National Research Centre (KNOW) for years 2014–2018, is acknowledged. AD is thankful to National Science Center, Poland, for funding and for supporting the scientific researches (UMO-2015/17/NST4/03804). GCD is supported by NSERC through a NSERC CGS-D award. Authors are thankful to Dr. Marcin Nyk (Department of Advanced Materials Engineering and Modelling, Faculty of Chemistry, Wrocław University of Technology) for performing scanning electron microscope experiments and MSc Martyna Zalewska for technical support.

References

- Alam, Md. N., Das, S., Batuta, S., Roy, N., Mandal, D., Begum, N.A., 2014. *Muraya koenigii* Spreng. leaf extract: an efficient green multifunctional agent for the controlled synthesis of Au nanoparticles. *ACS Sustain. Chem. Eng.* 2, 652–664.
- Rajathi, F. Arockiya Aarthi, Arumugam, R., Saravanan, S., Anantharaman, P., 2014. Phytosynthesis of gold nanoparticles assisted by leaves of *Suaeda monoica* and its free radical scavenging property. *J. Photochem. Photobiol. B* 135, 75–80.
- Baker, S., Rakshith, D., Kavitha, K.S., Santosh, P., Kavitha, J.U., Rao, Y., Satish, S., 2013. Plants: emerging as nanofactories towards facile route in synthesis of nanoparticles. *Bioimpacts* 3, 111–117.
- Basavegowda, N., Idhayadhulla, A., Rok, Y., 2014. Phyto-synthesis of gold nanoparticles using fruit extracts of *Hoveniadelphicis* and their biological activities. *Ind. Crop. Prod.* 52, 745–751.
- Bhambure, R., Bule, M., Shaligram, N., Kamat, M., Singhal, R., 2009. Extracellular biosynthesis of gold nanoparticles using *Aspergillus niger*- its characterization and stability. *Chem. Eng. Technol.* 32, 1036–1041.
- Bratescu, M.A., Cho, S.P., Takai, O., Saito, N., 2011. Size-controlled gold nanoparticles synthesized in solution plasma. *J. Phys. Chem. C* 115, 24569–24576.
- Cho, S.P., Bratescu, M.A., Saito, N., Takai, O., 2011. Microstructural characterization of gold nanoparticles synthesized by solution plasma processing. *Nanotechnology* 22, 455701.
- Cole, L.E., Ross, R.D., Tilley, J.M.R., Vargo-Gogola, T., Roeder, R. K., 2015. Gold nanoparticles as a contrast agents in X-ray imaging and computed tomography. *Nanomedicine* 10, 321–341.
- Daniel, M.C., Astruc, D., 2004. Gold nanoparticles assembly supermolecular chemistry, quantum-size related properties and applications toward biology, catalysis and nanotechnology. *Chem. Rev.* 104, 293–346.
- Das, R.S., Singh, B., Mukhopadhyay, S., Benerjee, R., 2012. Gold nanoparticles catalyzed oxidation of hydrazine by a metallo-superoxide complex: experimental evidences for surface activity of gold nanoparticles. *Dalton Trans.* 41, 4641–4648.
- Dhamecha, D., Jalalpure, S., Jadhav, K., 2016. *Nepenthes khasiana* mediated synthesis of stabilized gold nanoparticles: characterization and biocompatibility studies. *J. Photochem. Photobiol. B* 154, 108–117.
- Duan, H., Wang, D., Li, Y., 2015. Green chemistry for nanoparticle synthesis. *Chem. Soc. Rev.* 44, 5778–5792.
- Dzimitrowicz, A., Jamroz, P., Greda, K., Nowak, P., Nyk, M., Pohl, P., 2015a. The influence of stabilizers on the production of gold nanoparticles by direct current atmospheric pressure glow microdischarge generated in contact with liquid flowing cathode. *J. Nanopart. Res.* 17, 185.
- Dzimitrowicz, A., Lesniewicz, T., Greda, K., Jamroz, P., Nyk, M., Pohl, P., 2015b. Production of gold nanoparticles using atmospheric pressure glow discharge generated in contact with a flowing liquid cathode – a design of experiments study. *RSC Adv.* 5, 90534.
- El-Kassass, H.Y., El-Sheekh, M.M., 2014. Cytotoxic activity of biosynthesized gold nanoparticles with an extract of the red seaweed *Corallina officinalis* on the MCF-7 human breast cancer cell line. *Asian Pac. J. Cancer Prev.* 15, 4311–4317.
- Elia, P., Zach, R., Hazan, S., Kolusheva, S., Porat, Z., Zeiri, Y., 2014. Green synthesis of gold nanoparticles using plant extract as reducing agents. *Int. J. Nanomed.* 9, 4007–4021.
- Fierascu, R.C., Ion, R.M., Dumitriu, I., 2010. Noble metal nanoparticle synthesis in plant extracts. *Optoelectron. Adv. Mater.* 4, 1297–1300.
- Hainfeld, J.F., Dilmanian, F.A., Slatkin, D.N., Smilowitz, H.M., 2008. Radiotherapy enhancement with gold nanoparticles. *J. Pharm. Pharmacol.* 60, 977–985.
- Hao, E., Schatz, G.C., 2004. Electromagnetic fields around silver nanoparticles and dimmers. *J. Chem. Phys.* 120, 357–366.
- Heo, Y.K., Lee, S.Y., 2011. Effects of the gap distance on the characteristics of gold nanoparticles in nanofluids synthesized using solution plasma processing. *Met. Mater. Int.* 17, 431–434.
- Hieda, J., Saito, N., Takai, O., 2008. Exotic shapes of gold nanoparticles synthesized using plasma in aqueous solution. *J. Vac. Sci. Technol. A* 26, 854–856.
- Huang, X., Wu, H., Liao, X., Shi, B., 2010. One-step, size-controlled synthesis of gold nanoparticles at room temperature using plant tannin. *Green Chem.* 12, 395–399.
- Huang, X., Li, Y., Zhong, X., 2014. Effect of experimental conditions on size control of Au nanoparticles synthesized by atmospheric microplasma electrochemistry. *Nanoscale Res. Lett.* 9, 572.

- Hussain, I., Singh, N.B., Singh, A., Singh, H., Singh, S.C., 2016. Green synthesis of nanoparticles and its potential application. *Biotechnol. Lett.* 38, 545–560.
- Jain, K.K., 2007. Applications of nanobiotechnology in clinical diagnostics. *Clin. Chem.* 53, 2002–2009.
- Jia, H., Gao, X., Chen, Z., Liu, G., Zhang, X., Yan, H., Zhou, H., Zheng, L., 2012. The high yield synthesis and characterization of gold nanoparticles with superior stability and their catalytic activity. *CrystEngComm* 14, 7600–7606.
- Joseph, S., Mathew, B., 2014. Microwave assisted green synthesis of silver and gold nanocatalysts using the leaf extract of *Aerva lanata*. *Spectrochim. Acta A* 136, 1371–1379.
- Karthick, V., Kumar, V.G., Dhas, T.S., Govindaraju, K., Sinha, S., Singaravelu, G., 2015. Biosynthesis of gold nanoparticles and identification of capping agent using gas chromatography–mass spectrometry and matrix assisted laser desorption ionization–mass spectrometry. *J. Nanosci. Nanotechnol.* 15, 4052–4057.
- Khalil, M.M.H., Ismail, E.H., El-Magdoub, F., 2012. Biosynthesis of Au nanoparticles using olive leaf extract. *Arab. J. Chem.* 5, 431–437.
- Klekotko, M., Matczyszyn, K., Siednienko, J., Olesiak-Banska, J., Pawlik, K., Samoc, M., 2015. Bio-mediated synthesis, characterization and cytotoxicity of gold nanoparticles. *Phys. Chem. Chem. Phys.* 17, 29014–29019.
- Krishnaraj, C., Muthukumar, P., Ramachandran, R., Balakumar, M.D., Kalaichelvan, P.T., 2014. *Acalypha indica* Linn: Biogenic synthesis of silver and gold nanoparticles and their cytotoxic effects against MDA-MB-231, human breast cancer cells. *Biotechnol. Rep.* 4, 42–49.
- Kuladeep, R., Joythi, L., Shadak Alee, K., Deepak, K.L.N., Narayana Rao, D., 2012. Laser-assisted synthesis of Au–Ag alloy nanoparticles with tunable surface plasmon resonance frequency. *Opt. Mater. Express* 2, 161–172.
- Kumar, V.G., Gokavarapu, S.D., Rejeswari, A., Dhas, T.S., Karthick, V., Kapadia, Z., Shrestha, T., Barathy, I.A., Roy, A., Sinha, S., 2011. Facile green synthesis of gold nanoparticles using leaf extract of antidiabetic potent *Cassia auriculata*. *Colloids Surf. B* 87, 159–163.
- Link, S., El-Sayed, M.A., 1999. Size and temperature dependence of the plasmon absorption of colloidal gold nanoparticles. *J. Phys. Chem. B* 103, 4212–4217.
- Maximova, K., Aristova, A., Sents, M., Kabashin, A.V., 2015. Size-controllable synthesis of bare gold nanoparticles by femtosecond laser fragmentation in water. *Nanotechnology* 26, 065601.
- MubarakAli, D., Tahjuddin, N., Jeganathan, K., Gunasekaran, M., 2011. Plant extract mediated synthesis of silver and gold nanoparticles and its antibacterial activity against clinically isolated pathogens. *Colloid. Surf. B* 85, 360–365.
- Murphy, C.J., Gole, A.M., Stone, J.W., Sisco, P.N., Alkilany, A.M., Goldsmith, E.C., Baxter, S.C., 2008. Gold nanoparticles in biology: beyond toxicity to cellular imaging. *Acc. Chem. Res.* 41, 1721–1730.
- Murugan, K., Benelli, G., Panneerselvam, C., Subramaniam, J., Jeyalalitha, T., Dinesh, D., Nicoletti, M., Hwang, J.S., Suresh, U., Madhiyazhagan, P., 2015. *Cymbopogon citratus*-synthesized gold nanoparticles boost the predation efficiency of copepod *Mesocyclops aspericornis* against malaria and dengue mosquitoes. *Esp. Parasitol.* 153, 129–138.
- Olesiak-Banska, J., Gordel, M., Kolkowski, R., Matczyszyn, K., Samoc, M., 2012. Third-order nonlinear optical properties of colloidal gold nanorods. *J. Phys. Chem. C* 116, 13731–13737.
- Pal, N.B., Krysch, C., 2015. A facile one-pot synthesis of blue and red luminescent thiol stabilized gold nanoclusters: a thorough optical and microscopy study. *Phys. Chem. Chem. Phys.* 17, 21423–21431.
- Pasca, R.D., Mocanu, A., Cobzac, S.C., Petean, I., Horovitz, O., Tomoaia-Cotisel, M., 2014. Biogenic synthesis of gold nanoparticles using plant extracts. *Particul. Sci. Technol.* 32, 131–137.
- Patra, S., Mukherjee, S., Barui, A.K., Ganguly, A., Sreedhar, B., Patra, C.R., 2015. Green synthesis, characterization of gold and silver nanoparticles and their potential application for cancer therapeutics. *Mater. Sci. Eng. C* 53, 298–309.
- Pimpang, P., Chooapun, S., 2011. Monodispersity and stability of gold nanoparticles stabilized by using polyvinyl alcohol. *Chiang Mai J. Sci.* 38, 31–38.
- Saha, K., Bajaj, A., Duncan, B., Rotello, V., 2011. Beauty is skin deep: a surface monolayer perspective on nanoparticle interactions with cells and bio-macromolecules. *Small* 7, 1903–1918.
- Saito, N., Hieda, J., Takai, O., 2009. Synthesis process of gold nanoparticles in solution plasma. *Thin Solid Films* 518, 912–917.
- Sharma, B., Purkayastha, D.D., Hazra, S., Thajamanbi, M., Bhattacharjee, C.R., Ghosh, N.N., Rout, J., 2014. Biosynthesis of gold nanoparticles using a fresh water green alga, *Prasiola crispa*. *Mater. Lett.* 116, 94–97.
- Shirai, N., Uchida, S., Tochikubo, F., 2014. Synthesis of metal nanoparticles by dual plasma electrolysis using atmospheric dc glow discharge in contact with liquid. *Jpn. J. Appl. Phys.* 53, 046202.
- Singh, S., Sharma, V., Naik, P.K.R., Khandelwal, V., Singh, H., 2011. A green biogenic approach for synthesis of gold and silver nanoparticles using *Zingiber officinale*. *Dig. J. Nanomater. Biostruct.* 6, 535–542.
- Singh, P., Kim, Y.J., Yang, D.C., 2015. A strategic approach for rapid synthesis of gold and silver nanoparticles by Panax ginseng leaves. *Artif. Cells Nanomed. Biotechnol.* 24, 1–9.
- Singh, P., Kim, Y.-J., Zhang, D., Yang, D.-C., 2016. Biological synthesis of nanoparticles from plants and microorganisms. *Trends Biotechnol.* <http://dx.doi.org/10.1016/j.tibtech.2016.02.006>.
- Song, J.Y., Jang, H.-K., Kim, B.S., 2009. Biological synthesis of gold nanoparticles using *Magnolia kobus* and *Diopyros kaki* leaf extracts. *Process Biochem.* 44, 1133–1138.
- Stratil, P., Klejduš, B., Kubán, V., 2006. Determination of total content of phenolic compound and their antioxidant activity in vegetables – evaluation of spectrophotometric methods. *J. Agric. Food. Chem.* 54, 607–616.
- Suman, T.Y., Rajasree, S.R., Ramkumar, R., Rajthilak, C., Perumal, R., 2014. The Green synthesis of gold nanoparticles using an aqueous root extract of *Morinda citrifolia* L. *Spectrochim. Acta A* 118, 11–16.
- Tochikubo, F., Shimokawa, Y., Shirai, N., Uchida, S., 2014. Chemical reactions in liquid induced by atmospheric pressure dc glow discharge in contact with liquid. *Jpn. J. Appl. Phys.* 53, 126201.
- Wei, Z., Liu, C.J., 2011. Synthesis of monodisperse gold nanoparticles in ionic liquid by applying room temperature plasma. *Mater. Lett.* 65, 353–355.
- Yallappa, S., Manjanna, J., Dhananjaya, B.L., 2015a. Phytosynthesis of stable Au, Ag and Au–Ag alloy nanoparticles using *J. sambac* leaves extract, and their enhanced antimicrobial activity in presence of organic antimicrobials. *Spectrochim. Acta A* 137, 236–243.
- Yallappa, S., Manjanna, J., Dhananjaya, B.L., Vishwanatha, U., Ravishankar, B., Gururag, H., 2015b. Phytosynthesis of gold nanoparticles using *Mappia foetida* leaves extract and their conjugation with folic acid for delivery of doxorubicin to cancer cells. *J. Mater. Sci. Mater. Med.* 26, 235.
- Yan, T., Zhong, X., Rider, A.E., Lu, Y., Furman, S.A., Ostrikov, K., 2014. Microplasma-chemical synthesis and tunable real-time plasmonic responses of alloyed Au_xAg_{1-x} nanoparticles. *Chem. Commun.* 50, 3144–3147.